RSC Advances

Fluorescent organic ion pairs based on berberine: Counter-ion effect on the formation of particles and on the uptake by colon cancer cells

Journal:	*RSC Advances*
Manuscript ID:	RA-ART-09-2014-009993.R2
Article Type:	Paper
Date Submitted by the Author:	19-Nov-2014
Complete List of Authors:	Soulié, Marine; CNRS, ITAV, USR 3505 Frongia, Céline; CNRS, ITAV, USR 3505 Lobjois, Valérie; CNRS, ITAV, USR 3505 Fery-Forgues, Suzanne; ITAV, USR 3505

Fluorescent organic ion pairs based on berberine: Counter-ion effect on the formation of particles and on the uptake by colon cancer cells

Marine Soulié,[a,b] Céline Frongia,[a,b] Valérie Lobjois [a,b] and Suzanne Fery-Forgues [a,b,c,d] *

KEYWORDS. Berberine; organic salt; ion pair; cell uptake; fluorescence; nanoparticle

ABSTRACT. Four organic salts of berberine, a natural alkaloid, were prepared, characterized and studied for their fluorescence properties in solution and in the solid state. Aqueous suspensions of salt-based nanoparticles (NPs) were generated using the ion association technique. The amount and size of formed NPs were examined by UV-vis absorption spectroscopy, dynamic light scattering and transmission electron microscopy. They were closely dependent upon the nature of the salt and the experimental conditions of preparation. For instance, the four organic salts formed NPs in water, while only the tetraphenylborate salt (Ber^+TPB^-) was shown to give stable particles in the cell culture medium, i.e. Opti-MEM supplemented by fetal calf serum. The behavior of these salts placed in contact with cells was investigated. All berberine salts entered the cells and were detected in reticulum and mitochondria. However, the cell fluorescence was much stronger for Ber^+TPB^- than for the other salts. It could not be ascertained whether this effect was attributable to the intrinsic chemical properties of the Ber^+TPB^- salt or to the presence of nanoparticles. The nature of the anion also influenced the dye diffusion within the cells under illumination. A strong

phototoxic effect was observed. This study showed the interest of using organic salts for improved uptake of active compounds, and underlined the potential of carrier-free nano- and submicrometric particles for therapy, phototherapy and diagnosis.

1. Introduction

Delocalized lipophilic cations (DLCs) have for a long time attracted special attention as new potential chemo- and phototherapeutic agents for treatment of cancer.[1] These compounds are concentrated by cells and accumulate in mitochondria in response to negative inside transmembrane potentials. Since these potentials are much higher in cancer cells than in normal cells, some selectivity is therefore possible. Cell killing results from the inhibition of metabolic activity of mitochondria. Various DLCs such as rhodamine and rhodacyanine dyes, carbocyanines, tetraphenylphosphonium and Victoria blue BO have been investigated for this purpose. Many of these compounds showed significant anti-tumor activity on small animals, and one of them even lead to phase II clinical trials for treatment of carcinoma.[2] However, like for conventional chemotherapeutic agents, the development of DLCs is limited by their poor water solubility and the lack of adapted formulation approach that results in low efficacy at the approved dosage.

A clever way to bypass these difficulties would be to use DLCs as carrier-free nanoparticles (NPs), also called nanodrugs, which are now considered as a promising alternative to improve the biodistribution and bioavailability of cancer drugs [3] and cancer phototherapy agents.[4] Nanodrugs consist exclusively of pharmacologically active

compounds.[5] They have many advantages. Using drugs in the solid state obviates the need to dissolve poorly soluble compounds. The dense, solid state insures high chemical stability and maximal mass per volume loading. Additionally, the size of nanodrugs makes them big enough to escape renal clearance while being small enough to circulate in the blood stream and enter the tissues. The chemical nature of DLCs is well adapted to the preparation of carrier-free nanodrugs. Indeed, DLCs can be associated to organic counter-ions to give organic salts, the hydrophobicity of which allows the preparation of NPs in aqueous suspensions, potentially usable in biological medium. The system has the advantage of simplicity and versatility. The preparation of NPs made from organic salts does not require sophisticated formulation technologies, whether the salts are formed *in situ* by mixing aqueous solutions of cation and anion,[6] or formed in advance and then precipitated by an abrupt solvent change.[7, 8] The physical characteristics of the NPs obtained by both methods strongly depend on experimental parameters. Above all, the NP properties vary with the nature of the counter-ions. Since the latter are easily interchangeable, various NPs can be prepared, thus reducing the effort in synthesis and enhancing the potential of the drug for possible application.[9]

Curiously, the effect of counter-ions on the formation and activity of NPs made from DLCs has rarely been investigated. However, it is clear that the nature of the counter-ion plays a major role on the particle size and shape. It governs the solubility and the surface properties. A few studies, dealing with different types of organic salts where DLCs are fluorescent dyes, have brought some information on this topic.[6, 8, 9] From a biological viewpoint, the successful cellular uptake of cyanine dye, after introduction of cyanine^{+}AOT^{-}-based NPs in the culture medium has been first reported by Bwambok *et al.*, suggesting the interest of the system for biomedical use.[10] Recently, Magut *et al.* have examined the behavior of various Rhodamine 6G-based organic salts and they have shown that both the

anion and cation played an important and cooperative role in the antitumor properties of these compounds.[11] However, the biological behavior of organic salt-based NPs is almost unexplored. This obvious lack of data prompted us to undertake the present study, the aim of which was to clarify the influence of the counter-ion on the controlled preparation of NPs and the cellular uptake of the DLC salts.

Berberine is a perfect example of DLC. Hence, it seemed to be a good candidate to carry out this study. This compound is a natural alkaloid [12, 13] that possesses a wide range of pharmacological and biochemical activities,[14] including as anti-cancer agent.[15, 16] It is well known for its photochemical activity [17] and has been proposed for use in cancer phototherapy.[18, 19] Berberine is also a brightly coloured cation, that is moderately fluorescent in organic solvents,[20] lipid phases,[21] constrained media,[22] and in the solid state,[7] allowing investigations by UV-vis absorption and fluorescence spectroscopies. In a previous work, we synthesized a fluorescent organic salt formed with the aromatic berberine cation (Ber^+) and the long-chain palmitate anion (Pal^-), and this compound was used to prepare aqueous suspensions of fluorescent nanofibers via the reprecipitation method.[7] In the present study, berberine was once again associated to palmitate, as well as to dioctylsulfosuccinate (AOT^-), tosylate (Tos^-), also called *p*-toluenesulfonate, and tetraphenylborate (TPB^-) (Fig. 1). The four anions differed by the nature of the charged group (carboxylate, sulfonate and borate) and hydrophobic moiety that passed from aliphatic to polyaromatic. Our aim was first to examine whether these salts can give particles, possibly with controlled size and improved consistency, and secondly to test the way they interact with living cells. It must be noticed that in all this work, berberine salts were written as Ber^+X^-, whatever their dissociation state. “Nanoparticle” was also used as a generic term for nanometric and submicrometric particles, as it is often the case for organic compounds.

Figure 1

Figure 1. Chemical structures of berberine cation (Ber^+) and associated anions: palmitate (Pal^-), dioctylsulfosuccinate (AOT^-), tosylate (Tos^-) and tetraphenylborate (TPB^-). Berberine position numbering was made according to ref. 13.

2. Results

2.1. Synthesis and characterization of the berberine organic salts

Before undertaking the preparation of NPs, the composition of berberine organic salts was studied on macroscopic amounts. The salts were obtained by mixing the sodium salt of the desired anion (Na^+X^- with X^- = Pal^-, AOT^-, Tos^- and TPB^-), previously dissolved in water, with a concentrated aqueous solution of berberine chloride (Ber^+Cl^-) (see experimental section). A bright yellow precipitate readily appeared, due to the poor solubility of the formed organic salt. This precipitate was collected by filtration or centrifugation, extensively rinsed with water to remove inorganic salts, and dried at 50°C under vacuum. The characterization was made by mass spectrometry (electrospray ionization technique, positive and negative modes) and ^1H NMR spectroscopy. The berberine NMR signals were attributed according to literature data.[13] For the four salts, the integration indicated that the organic anion and the berberine cation were in 1:1 stoichiometric proportion. For Ber^+TPB^-, the NMR spectra were recorded in $CDCl_3$ instead of CD_3OD for solubility reasons. The berberine protons H4, H5 and H6 of this compound were markedly shifted upfield with respect to the other salts. This shift was too important to arise only from a solvent effect and it was attributed to the formation of a contact ion pair between the berberine cation and the large tetraphenylborate anion. It was

likely that the aromatic ring current of TPB^- affected the NMR signals of the protons located close to N^+, as reported for various anilinium cations in chlorohydrocarbons for which TPB^- has been introduced as an NMR shift reagent.[23]

2.2. Optical properties

First of all, the optical properties of the four salts were investigated in dilute organic solutions at concentrations around 10 μM. Acetonitrile was chosen as the solvent to insure full dissolution of the organic salts. The obtained solutions were crystal clear. They all exhibited the characteristic UV-vis absorption spectrum of berberine cation, with maxima at 232, 266, 346 and 428 nm, the long-wavelength band being of much weaker intensity than the other ones (Fig. S1†). The shape of the fluorescence emission spectra did not depend on the excitation wavelength and the maxima were at 554 nm whatever the counter-ion (Fig. 2a). The absorption and fluorescence spectra of the organic salts were identical to those of berberine chloride in acetonitrile. This similarity indicated that all organic salts were dissociated in this solvent in the 10^{-5} M range and the anion had no influence on the spectroscopic properties. Regarding the emission efficiency, the dissolved compounds were moderately emissive. This observation was in line with the fluorescence quantum yield value of Ber^+Cl^- in acetonitrile that has been reported to be 0.021. [20]

The emission properties were then investigated on the powders. The four organic salts and Ber^+Cl^- were found to be emissive in the solid state. The photoluminescence spectra were blue-shifted and narrow with respect to solutions. Their position depended on the nature of the anion, with a maximum between 512 and 552 nm (Fig. 2b). The quantum yields of the powder solids ranged from 0.052 for Ber^+AOT^- to 0.006 for Ber^+TPB^- (Supporting Information Table

S1). Berberine salts were thus moderately emissive both in organic solvents and in the solid state.

Figure 2

Figure 2. a) Normalized fluorescence emission spectra of the berberine salts dissolved in acetonitrile at around 1×10^{-5} M, λ_{ex} = 430 nm; b) Normalized photoluminescence spectra of the powder microcrystalline compounds. λ_{ex} = 420 nm. Ber^+Pal^-, orange lines; Ber^+AOT^-, purple lines; Ber^+Tos^-, red lines; Ber^+TPB^-, green lines; Ber^+Cl^-, blue lines.

2.3. Controlled preparation and morphological properties of nanoparticles

Nanoparticles were prepared *in situ* using the "ion-association technique".[6] Solutions of the four organic anions as their sodium salt (Na^+X^- with X^- = Pal^-, AOT^-, Tos^- and TPB^-) were mixed with solutions of berberine chloride in equimolar proportion. Preparation was made either in water or in Opti-MEM cell culture medium that contains various electrolytes, phenol red, antibiotics and proteins, and was thus prone to interfere with the NP formation and stability. Moreover, in order to test the influence of the preparation method on the NP size, two different protocols were followed (cf. Experimental section). According to Protocol 1, the organic salts were generated from a concentrated mixture of their inorganic precursors in water and, after equilibration, the mixture was diluted 10 folds with water or Opti-MEM. According to Protocol 2, the organic salts were formed directly by mixing dilute solutions of precursors. Comparison was made with berberine chloride. Unless otherwise stated, the final concentration of berberine salts was comparable in all cases (50 μM).

UV-vis absorption spectroscopy allowed the aggregation state to be estimated. The salts formed in water were first considered. The spectrum of Ber^+Cl^- at 50 μM, used as a reference, displayed absorption maxima at 263, 344 and 421 nm. The extinction coefficient value (ε = 4800 $M^{-1}cm^{-1}$at 421 nm) indicated that a large proportion of this species was dissolved, by comparison with literature data.[20] When Protocol 1 was followed, the spectra of Ber^+Tos^-, Ber^+AOT^- and Ber^+Pal^- had the same shape as that of Ber^+Cl^- (Fig. 3a), but their intensities were weaker. The hypochromic effect was attributed to the increasingly important formation of aggregates with passing from Ber^+Tos^- to Ber^+AOT^-, and then to Ber^+Pal^-. Using Protocol 2, the spectra of Ber^+Cl^- and Ber^+Tos^- were strictly superimposable (with ε = 5200 $M^{-1}cm^{-1}$ at 421 nm), and the spectra of Ber^+AOT^- and Ber^+Pal^- showed a hypochromic effect weaker than that previously noticed (Fig. 3b). This observation suggested that the formation of aggregates was reduced by using the second protocol.

The same experiments were carried out in Opti-MEM containing 5% fetal calf serum. Using Protocol 1, the spectra of Ber^+Cl^-, Ber^+AOT^- and Ber^+Tos^- were superimposable. Only the spectrum of Ber^+Pal^- showed a slight deviation of the baseline, due to diffusion of particles in suspension (Fig. 3c). Using Protocol 2, the four spectra were similar, indicating important dissolution of all these compounds in Opti-MEM.

Whatever the protocol used, the spectra of Ber^+TPB^- were shifted to the red with respect to the other salts, suggesting a strong interaction between berberine and the TPB^- anion (Fig. 3d). In most of the cases, the spectra were broadened and the baseline was strongly deviated upwards. This effect indicated the presence of a large number of aggregates. Weak variations were only observed when the salt was prepared in Opti-MEM according to Protocol 2.

Consequently, the formation of particles from Ber^+Tos^-, Ber^+AOT^- and Ber^+Pal^- was particularly sensitive to the experimental procedure and medium, while particles of Ber^+TPB^-

seemed to be much more robust. To confirm this observation, experiments were repeated according to Protocol 1 in Opti-MEM, with the salt concentration being reduced by half (25 μM). No significant aggregation effects were then detected for Ber^+Tos^-, Ber^+AOT^- and Ber^+Pal^-, while aggregation was still obvious for Ber^+TPB^- (Fig. S2†).

Figure 3

Figure 3. UV-vis absorption spectra of the berberine salts prepared in water according to a) Protocol 1 and b) Protocol 2. c) Spectra of the same compounds generated in Opti-MEM (5% fetal calf serum) according to Protocol 1. Ber^+Pal^-, orange lines; Ber^+AOT^-, purple lines; Ber^+Tos^-, red lines; Ber^+Cl^-, blue lines. d) Spectra of Ber^+TPB^- generated in water (green plain line) and Opti-MEM (green dashed line) according to Protocol 1, and in water (black plain line) and Opti-MEM (black dashed line) according to Protocol 2. Salt concentration: 50 μM.

Dynamic light scattering (DLS) was used to search the presence of NPs generated in water and in Opti-MEM (5% fetal calf serum) at 50, 25, and 2.5 μM according to Protocol 1 (Fig. 4). For Ber^+Pal^-, Ber^+AOT^- and Ber^+Tos^-, NPs were detected in water, at least at the two highest salt concentrations. The hydrodynamic diameter was increased with increasing salt concentration. The Ber^+Pal^- NPs formed in water at high salt concentration reached a diameter of 450 nm. In Opti-MEM, the presence of NPs was not obvious for these three salts, because the signal was equivalent to that of the medium alone. In contrast, Ber^+TPB^- formed NPs, whatever the medium and even at low concentration. With one exception, the Ber^+TPB^- particles had the same size, around 250 nm.

Figure 4

Figure 4. Hydrodynamic diameter (in intensity) of NPs measured by DLS. Berberine salts were prepared a) in water and b) in Opti-MEM (5% fetal calf serum) according to Protocol 1 at three salt concentrations: 50 μM (dark bar), 25 μM (medium bar), and 2.5 μM (light bar).

The presence of particles was also ascertained by transmission electron microscopy (TEM). The grids observed by TEM correspond to suspensions of NPs generated with a salt concentration of 50 μM. For Ber^+Pal^-, Ber^+AOT^- and Ber^+Tos^-, only the NPs generated in water according to Protocol 1 were investigated. For Ber^+TPB^-, the NPs were generated in water and in Opti-MEM according to the two preparation modes. All these samples were heterogeneous and contained a small number of microcrystals. Particles of Ber^+AOT^- appeared like sort of sheets that were torn longitudinally. The samples of Ber^+Tos^- and Ber^+Pal^- showed a population of thin elongated NPs that were about 50-60 nm long and frequently agglomerated by the side of each other (Fig. S3†). The same type of particle was found for Ber^+TPB^- in water, whatever the protocol used. In the latter case, an attempt to get an electron diffraction pattern resulted in a halo, suggesting that NPs were polycrystalline. Elongated NPs of Ber^+TPB^- in water coexisted with a large number of submicroscopic crystals that measured between 100 and 300 nm (Fig. 5a), or less, with a tendency to agglomerate (Fig. 5b). In Opti-MEM, elongated NPs were no longer distinguished. Only spherical agglomerates were observed, probably formed by small elongated particles, but it was not possible to say if they were made of Ber^+TPB^- or resulted from artefacts due to the complexity of the medium.

TEM showed that the general trend of berberine salts was to form elongated NPs in water, whatever the counter-ion. This observation was strongly reminiscent of the nanofibers obtained with Ber^+Palm^- using the reprecipitation method.[7] It must be noted that the elongated NP shape can make DLS results somewhat imprecise. The difference between Ber^+TPB^- and

the other salts was in the larger amount of formed NPs, and in the presence of many submicroscopic crystals with a size between 100 and 300 nm. The TEM and DLS results would then be in line: the submicroscopic crystals of Ber^+TPB^- were probably responsible for the peak at 250 nm. The microcrystals that were present in every suspension were not taken into account by DLS.

Figure 5

Figure 5. Transmission electron microscopy images of Ber^+TPB^- in water at 50 μM prepared according to Protocol 1.

2.4. Stability of nanoparticles.

The stability of the suspensions over time was examined. To do so, berberine salts were generated at the concentration of 50 μM using Protocol 1 that favored the formation of NPs. Samples were first prepared in water and left to stand at 25°C under gentle stirring. The hydrodynamic diameter of NPs was measured every 30 min during 3 h, and then after 24h. In these conditions, no significant variations of the NP diameter were observed for Ber^+TPB^-, showing an excellent stability of these particles. For Ber^+Pal^-, the particle average diameter was around 350 nm. The size was increased during the first two hours, and then little variations were observed after 24h (Fig. S4†). Ber^+AOT^- particles appeared to be instable, due to a trend to agglomeration visible on the walls of the eppendorf, while Ber^+Tos^- particles rapidly dissolved.

Stability was then checked in Opti-MEM in the absence of fetal calf serum at 37°C, for Ber^+TPB^- and Ber^+Pal^- salts. Particles of Ber^+TPB^- were again perfectly stable for 1h. For Ber^+Pal^-, the size of the particles initially measuring 230 nm was slightly reduced over time.

At this stage, it seemed instructive to investigate the influence of proteins on the berberine salts. The UV-vis absorption spectra of Ber^+Cl^- at 50 μM in water and in Opti-MEM (containing 5% fetal calf serum) were almost superimposable (Fig. S5†). No shift indicating possible interactions of the dissolved compound with electrolytes or proteins of Opti-MEM could be detected. The possible influence of proteins on the NP size was then regarded. Particles of Ber^+Pal^- were generated in Opti-MEM containing 5% fetal calf serum and incubated at 37°C. After 1h, no particles with a diameter above 100 nm were detected by DLS, and this indicated an evolution of the sample in the presence of proteins. In the same conditions, particles of Ber^+TPB^- were stable after 3h incubation (Fig. S6†). For the sake of comparison, samples of Ber^+TPB^- particles were also prepared with 10% fetal calf serum in Opti-MEM. They were examined immediately and after 1h incubation at 37°C by DLS, as well as by UV-vis absorption and fluorescence spectroscopies. DLS indicated a very weak increase of the particle diameter with increasing the serum content (Fig. S7†). The general shape of the absorption spectra was hardly changed, so that no new type of interaction was detected (Fig. S8†). The fluorescence spectra showed a weak dissolution of berberine in the medium with no clear link with the serum content (Fig. S9†). The effect of proteins on Ber^+TPB^- NPs was therefore weak.

2.5. Cellular uptake

The cytotoxicity of berberine palmitate was evaluated on the HCT-116 human colorectal adenocarcinoma cell line. Cell viability was not significantly altered when up to 10 μM Ber^+Pal^- was added to the culture medium (Supporting Information Fig. S10†). Throughout the following biology work, it was also observed that cell viability was identical in the absence and presence of every berberine salt used at the concentration of 50 μM, as long as the samples were kept in the dark.

The cell uptake of the berberine organic salts was then assessed on living cells. Salts were prepared using Protocol 1. Precursors were mixed at high concentration, and were then diluted in Opti-MEM (5% fetal calf serum) at the final concentrations in organic salt of 50 μM, 25 μM or 2.5 μM. Cells were incubated in the presence of salts for 1h before live imaging (λ_{ex} = 438 nm). As shown in Figure 6, cells readily became fluorescent, which suggested internalization of the dye (Fig. 6). A striking difference appeared with the salt concentration used and the nature of the counter-ion. For Ber^+Cl^-, Ber^+Pal^-, Ber^+AOT^- and Ber^+Tos^- at 2.5 and even 25 μM, the cell fluorescence was very weak. At 50 μM, the cell fluorescence was of moderate intensity, and roughly comparable for every salt. In contrast, for Ber^+TPB^-, cell fluorescence was detected at low salt concentration and was intense at high concentration. Fluorescence was still visible 24h after incubation (data not shown).

Figure 6

Figure 6. HCT-116 cells incubated during 1h in the presence of the indicated concentration of berberine salts. Images correspond to the fluorescence signal obtained with λ_{ex} = 438 nm and λ_{em} = 525 nm (±25 nm). Scale bar: 20 μm.

Granular fluorescence from berberine salts was observed within the cytoplasm. Careful examination of the images even suggested that fluorescence could arise from mitochondria (Supporting Information Fig. S11†). To determine precisely the origin of fluorescence, additional experiments were conducted using Ber^+TPB^- that produced the clearest images. Cells membranes were stained by a red emitting dye (Cell Mask®). They were incubated with 50 μM of Ber^+TPB^-. The red fluorescence signals coming from plasma membranes, and the green fluorescence signal from berberine were collected on different

channels. Comparison of these data confirmed that green fluorescence was preferentially located in the perinuclear region of the cells and exclusively emitted from the cytoplasm. No accumulation in the nucleus or in cytoplasmic membrane was observed (Fig. 7a).

Co-staining was then examined on cells treated with kit ER-ID Red® or MitoTracker® Red CMXRos, two markers that specifically label endoplasmic reticulum and mitochondria, respectively. In both cases, the green fluorescence of berberine was superimposable with the red fluorescence of these dyes (Fig. 7b and 7c).

Figure 7

Figure 7. HCT-116 cells stained with a) Cell Mask®, b) kit ER-ID Red® and c) MitoTracker® Red CMXRos, and then incubated during 1h with Ber^+TPB^- (50 μM). Fluorescence signal obtained with λ_{ex} = 470 nm and λ_{em} = 525 nm for left images (Ber^+TPB^- fluorescence); λ_{ex} = 550 nm and λ_{em} = 605 nm for center images (red markers fluorescence); Right images: merged. Scale bar: 10 μm.

Cells incubated with berberine salts were viable for a long time in the dark. However, prolonged observation of cells incubated with berberine salts gave evidence for their mortality under illumination by the microscope light beam. The viability of cells incubated in the absence of berberine was apparently not altered in the same conditions. A comparison was made with HCT-116 cells placed in the presence of Ber^+Cl^- and Ber^+TPB^- (50 μM) for 1h before washing, and repeatedly observed every 20 s. At the beginning of the observation, fluorescence spots were bright and well distinct, concentrated in mitochondria and reticulum. Then, progressively, fluorescence became diffuse in the whole cytoplasm and the cell contours were blurred (Fig. 8). Qualitatively, the process seemed to be identical for both

berberine salts. However, the diffusion of the fluorophore in the cells seemed to be slower for Ber^+TPB^- than for Ber^+Cl^-. It was checked that irradiation with light at 470 nm for the same period of time in the absence of berberine salts caused only minor damage to the cells, by comparison with what was observed in the presence of salts (Fig. S12†).

Figure 8

Figure 8. Videomicroscopy images of HCT-116 cells incubated at 37°C for 1h with Ber^+Cl^- (top) and Ber^+TPB^- (bottom) at the concentration of 50 μM in Opti-MEM, and then washed with Opti-MEM. 1 image every 20 s. λ_{ex} = 470 nm and λ_{em} = 525 nm. Scale bar: 20 μm.

3. Discussion

According to our previous measurements and literature data, berberine salts were known to be moderately fluorescent in solution, except in aqueous medium.[7, 17, 20] The present work showed that various berberine organic salts were also emissive in the solid state, with a photoluminescence quantum yield of the same order of magnitude as in organic solvents. The nature of the anion played a critical role in the solid-state spectroscopic properties, probably because counter-ions influence the molecular arrangement of the fluorophores in the solid state and modify the interactions between the latter.[9, 24] This effect will be discussed in detail using a large number of salts in a forthcoming paper. The important point here is that the ubiquitous fluorescence emission of berberine allowed this compound to be monitored after dissolution in a lipophilic phase, as well as in the solid state. It must also be underlined that the absorbance and fluorescence properties in solution were similar for every salt, so that the signals can be related to the same amount of berberine cation in every case.

The berberine salts were poorly soluble in aqueous medium and inclined to form nanometric and submicrometric particles. Their trend to aggregation was increased in the order: Ber^+Cl^- < Ber^+Tos^- < Ber^+AOT^- < Ber^+Pal^- << Ber^+TPB^-, as could be expected considering the hydrophobicity of the anion. Interesting differences were found according to the particle preparation mode. Observations made by UV-vis absorption spectroscopy and DLS were totally in line. From a general viewpoint, they indicated that a greater number of particles were formed when the salts were generated from a concentrated mixture of precursors, and then diluted (according to Protocol 1), than when the salts were directly formed from dilute solutions of precursors. It was readily understandable that high concentrations favored aggregation, but it was remarkable that the particles formed in concentrated medium remained stable for a time after dilution. The stability over time strongly depended on the nature of the counter-ion, the TPB^- anion giving by far the most stable particles. The salt solubility was expected to be different in water and in Opti-MEM, but the direction of the change was hard to predict. Opti-MEM contains a large amount of various electrolytes, which could compete for solvation by water molecules and promote aggregation of berberine organic salts due to a salting out effect. At the opposite, it was observed that the salt solubility was increased in this medium. Proteins reduced the stability of the fragile particles, although they had little impact on the very stable particles of Ber^+TPB^-. From a general viewpoint, these observations imply that developments made in water are not directly transposable to biological culture media.

For cell uptake experiments, berberine salts were prepared according to Protocol 1 in Opti-MEM. For Ber^+TPB^-, this procedure led to particles that measured about 250 nm and remained stable at 37°C over the incubation time. The presence of NPs could not be evidenced for the other salts, which were probably dissolved. It was observed that the most soluble salts led to a weaker fluorescence signal from the cells than Ber^+TPB^-. Four

hypotheses at least can be proposed to explain this observation. (i) According to their chemical nature, the berberine salts were differently distributed within the cells. For instance, $Ber^{+}TPB^{-}$ was mainly localized in the lipid membranes of the organelles, generating a strong fluorescence signal, while a proportion of the other salts, which are less hydrophobic, remained in the cytoplasm where their fluorescence was quenched by water molecules. Indeed, the fact that the cytoplasm was not fluorescent did not exclude the presence of berberine in this compartment. (ii) The distribution of all the salts in the cell compartments was similar, and the overall signal was thus proportional to the amount of berberine salt that had entered the cells. In this case, $Ber^{+}TPB^{-}$ would penetrate more easily into the cells than the other salts. (iii) The increased incorporation of $Ber^{+}TPB^{-}$ was linked to the presence of particles. This hypothesis suggests that particles could be internalized into cells by endocytosis. In this regard, organic dye NPs that measured less than 300 nm have been reported to enter the cells by endocytosis before dissolving in the phospholipid membranes.[25] It has also been shown that much bigger particles were internalized by cells.[26] In the present work, comparing the uptake of $Ber^{+}TPB^{-}$ particles generated by Protocol 1 and 2 did not allow significant differences in cell fluorescence to be evidenced. This suggests that the particle size was not the major parameter controlling the internalization process. (iv) Another possibility is that the $Ber^{+}TPB^{-}$ particles were trapped at the cell surface for affinity reasons, thus acting as a reservoir and increasing the local dye concentration.

There is no indication as to the diffusion of the dye after it had entered the cells. After internalization, all berberine salts led to the same type of fluorescent signal within the cells. The nature of the anion did not alter the capacity of the berberine cation to finally reach its target. The berberine fluorophores were detected in reticulum and mitochondria. This result was in line with the literature data, because the natural alkaloid $Ber^{+}Cl^{-}$ has been reported several times to be located in mitochondria where it causes various dysfunctions.[16, 27] It is

noteworthy that localization of the dye in other organelles, such as endosomes and lysosomes, was not tested but cannot be ruled out, as it is also the case for its presence in the cytoplasm.

Finally, it was observed that the viability of HCT-116 cells was rapidly decreased in the presence of berberine salts under illumination, suggesting that toxicity was of photochemical origin. The berberine cation has been reported many times to be photochemically active. Its phototoxicity has been related to the generation of singlet oxygen and superoxide anion radical.[16-19, 28] A striking feature of berberine photoreactivity is that this compound is a weak photosensitizer in water, while it produces reactive oxygen species very efficiently in a nonpolar environment and after electrostatic binding to DNA.[17, 18] A direct effect on mitochondrial DNA is most likely. A difference in the speed of dye diffusion within the cell was qualitatively noticed with the nature of the anion.

More detailed studies would be necessary to see how berberine salts were internalized by the cells. This process might depend on the nature of the organic counter-ion. It would also be interesting to know how long the organic counter-ions remained associated to the berberine cation after internalization. If the ion pair is stable over time, it could influence the interaction with biological molecules, with a possible effect on the pharmacological and photochemical activities of berberine. Whatever the mechanism, it is clear from this study that the nature of the salt deeply influenced the behavior of the dye with respect to the cells, the intensity of the fluorescence signal and the speed of the photochemical process.

4. Experimental section

Chemicals: Berberine chloride (9,10-dimethoxy-2,3-methylenedioxy-5,6-dihydrodibenzo[*a,g*] quinolizinium chloride) was purchased from Sigma and used as received.

Palmitic acid soldium salt (Fluka, 97%), dioctyl sulfosuccinate sodium salt (Aldrich, 98%), sodium *p*-toluenesulfonate (Aldrich, 95%) and sodium tetraphenylborate (Sigma-Aldrich, 99.5%) were used without further purification. High-pressure demineralized water (resistivity 18.3 MΩ.cm) was prepared with a Milli-Q apparatus (Millipore). Opti-MEM® I reduced serum medium, GlutaMAX^{TM} supplement, was purchased from Life Technologies and supplemented with penicillin, streptavidine and 5% fetal calf serum. In this work, this medium was designed by Opti-MEM. Variations in the content of fetal calf serum were indicated in the text.

Synthesis of berberine organic salts: A 2 mM stock solution was prepared by dissolving 0.185 g (5×10^{-4} mol) of berberine chloride (Ber^+Cl^-) in 250 mL of water. An aliquot (50 mL) of Ber^+Cl^- solution was then mixed with 50 mL of an aqueous solution of sodium palmitate (Na^+Pal^-) at 2 mM, as well as with 80 mL of solutions of sodium dioctylsulfosuccinate (Na^+AOT^-), sodium *p*-toluenesulfonate (Na^+Tos^-) and sodium tetraphenylborate (Na^+TPB^-) at 5 mM. The AOT^-, Tos^- and TPB^- anions were used in excess to promote precipitation of the organic salt. After one night under stirring, the formed precipitates of Ber^+Pal^- and Ber^+AOT^- were isolated by filtration on a Büchner apparatus. The precipitates of Ber^+Tos^- and Ber^+TPB^- were collected by centrifugation at 9000 rpm for 1h. In every case, the solid was extensively rinsed with water to remove excess inorganic salt and then dried under vacuum at 50°C, yielding the desired organic salt (17.7 mg Ber^+Pal^-, 33.9 mg Ber^+AOT^-, 14 mg Ber^+Tos^- and 25 mg Ber^+TPB^-) as a bright yellow powder.

Berberine palmitate (Ber^+Pal^-). ^{1}H NMR (CD_3OD): δ ppm = 0.91 (t, J = 6.5 Hz, 3H, CH_3), 1.30 (m, 24H, CH_2), 1.60 (m, J = 7.5 Hz, 2H, $C\underline{H}_2$-CH_2-COO^-), 2.16 (t, J = 7.5 Hz, 2H, CH_2-COO^-), 3.28 (t, J = 6.3 Hz, 2H, H5), 4.13 (s, 3H, C10-$OC\underline{H}_3$), 4.23 (s, 3H, C9-$OC\underline{H}_3$), 4.94 (t, J = 6.3 Hz, 2H, H6), 6.13 (s, 2H, O-CH_2-O), 6.98 (s, 1H, H4), 7.68 (s, 1H, H1), 8.02

(d, J = 9.1 Hz, 1H, H12), 8.14 (d, J = 9.1 Hz, 1H, H11), 8.73 (s, 1H, H13), 9.80 (s, 1H, H8). ES-MS: $[M]^+$ = 336.4; $[M]^-$ = 255.6.

Berberine dioctylsulfosuccinate (Ber^+AOT^-). ^1H NMR (CD_3OD): δ ppm = 0.85-0.92 (m, 12H, CH_3), 1.29-1.42 (m, 16H, CH_2), 1.50-1.61 (m, 2H, CH), 2.96 (d, J = 3 Hz, 0.35H, $OC(O)CH_2$), 3.01 (d, J = 3 Hz, 0.65H, $OC(O)CH_2$), 3.14 (d, J = 11.5 Hz, 0.65H, $OC(O)CH_2$), 3.19 (d, J= 11.5 Hz, 0.35H, $OC(O)CH_2$), 3.24 (t, J = 6.4 Hz, 2H, H5), 3.96-4.06 (m, 5H, CH-SO_3^- and CH_2-O), 4.07 (s, 3H, C10-OCH_3), 4.19 (s, 3H, C9-OCH_3), 4.92 (t, J = 6.4 Hz, 2H, H6), 6.08 (s, 2H, O-CH_2-O), 6.92 (s, 1H, H4), 7.57 (s, 1H, H1), 7.95 (d, J = 9.1 Hz, 1H, H12), 8.05 (d, J = 9.1 Hz, 1H, H11), 8.59 (s, 1H, H13), 9.73 (s, 1H, H8). ES-MS: $[M]^+$ = 336.3; $[M]^-$ = 421.3.

Berberine tosylate (Ber^+Tos^-). ^1H NMR (CD_3OD): δ ppm = 2.34 (s, 3H, Ph-CH_3), 3.24 (t, J = 6.4 Hz, 2H, H5), 4.09 (s, 3H, C10-OCH_3), 4.19 (s, 3H, C9-OCH_3), 4.91 (t, J = 6.4 Hz, 2H, H6), 6.09 (s, 2H, O-CH_2-O), 6.93 (s, 1H, H4), 7.17 (d, J = 7.8 Hz, 2H Ph), 7.61 (s, 1H, H1), 7.66 (d, J = 7.8 Hz, 2H Ph), 7.97 (d, J = 9.1 Hz, 1H, H12), 8.07 (d, J = 9.1 Hz, 1H, H11), 8.64 (s, 1H, H13), 9.71 (s, 1H, H8). ES-MS: $[M]^+$ = 336.3; $[M]^-$ = 171.0.

Berberine tetraphenylborate (Ber^+TPB^-). ^1H NMR ($CDCl_3$): δ ppm = 2.37 (t, J = 6.0 Hz, 2H, H5), 3.04 (t, J = 6.0 Hz, 2H, H6), 4.11 (s, 3H, C10-OCH_3), 4.20 (s, 3H, C9-OCH_3), 6.04 (s, 2H, O-CH_2-O), 6.58 (s, 1H, H4), 6.72 (t, J = 7.2 Hz, 4H), 6.90 (t, J = 7.2 Hz, 8H), 7.42-7.62 (m, H11, H12 and 8H from TPB^-), 7.80 (s, 1H, H1), 8.70 (s, 1H, H13), 8.72 (s, 1H, H8). ES-MS: $[M]^+$ = 336.3; $[M]^-$ = 319.2.

Apparatus and methods: Mass spectra were obtained with a Waters Auto Purif device using the electrospray ionization technique (Chemistry platform, ITAV). The NMR spectra were recorded on a Bruker AC300 spectrometer operating at 300.13 MHz (Service commun de RMN de l'Institut de Chimie de Toulouse, Université Paul Sabatier). The hydrodynamic diameter of nanoparticles was measured by dynamic light scattering (DLS) on a Malvern Zetasizer Nano ZS apparatus equipped with a 633-532 nm laser (BioNano platform, ITAV). Two distinct samples were used for each measurement, and scanning was repeated 10 times on each sample. Transmission electron microscopy was performed using a JEOL JEM 1400 apparatus (Service Commun de Microscopie Electronique de l'Université Paul Sabatier). To prepare the samples, some droplets of suspension were deposited on a carbon grid. The excess liquid was drawn off with paper. The samples were revealed with a droplet of ammonium molybdate solution (1% in water) and allowed to dry for 48h under vacuum at 50°C. All optical spectroscopy measurements were performed on a Xenius SAFAS spectrofluorometer equipped with a Hamamatsu R2658 detector. UV-vis absorption spectra were recorded using cells of 1cm optical pathway in a temperature-controlled compartment (20°C). For steady state fluorescence spectra, cells of 1 mm optical pathway were also used when necessary in order to keep absorbance below 0.1. Absorption of the TPB^- anion at short wavelengths was corrected. Photoluminescence spectra were recorded using a $BaSO_4$ integrating sphere and were corrected. Powder compounds were deposited on a metal support. To measure photoluminescence quantum yields, the excitation source was scanned in order to evaluate the reflected light for the empty sphere (L_a), the samples facing the source light (L_c) and the sample out of the irradiation beam (L_b). The fluorescence spectra were recorded with the sample facing the source light (E_c) and out from direct irradiation (E_b). The PM voltage was adapted to the measurement of reflected light and emission spectra, respectively, and

proper correction was applied to take into account the voltage difference. The absolute photoluminescence quantum yield values (Φ_P) were determined using the formula: [29]

$$\Phi_P = [E_c - (1 - \alpha)\, E_b] / L_a\, \alpha$$

with $\alpha = 1 - L_c / L_b$. The error on photoluminescence quantum yield was estimated to be 20%.

Nanoparticle preparation: NPs were prepared in high-pressure demineralized water and Opti-MEM medium.

Protocol 1. A solution of 150 µL Ber^+Cl^- at 1 mM in demineralized water was mixed with the same volume of an equimolar aqueous solution of the organic anion sodium salt. This concentrated mixture was sonicated for 15 min with an ultrasound bath and then left to stand at room temperature for 24h. The mixture was then diluted 10 fold by addition of appropriate volume of water or Opti-MEM, the concentration in organic salt being then 50 µM. Dilute solutions were immediately used. Protocol was adapted for the preparation of solutions at 25 µM and 2.5 µM (Supporting Information Table S2).

Protocol 2. A solution of 150 µL Ber^+Cl^- at 1 mM in demineralized water was diluted with 2.7 mL water or Opti-MEM. A volume of 150 µL of an equimolar solution of the organic anion sodium salt in water was then added. The concentration of organic salt was thus 50 µM. The mixture was used immediately after preparation.

Cell studies: Adenocarcinoma colorectal cell lines HCT-116 (ATCC CCL-247) were cultured as monolayers, in a humidified atmosphere with 5% CO_2 at 37°C, in Dulbecco's

modified Eagle medium (Gibco) supplemented with 10% fetal calf serum (Gibco), penicillin and streptomycin.

Cytotoxicity of $Ber^{+}Pal^{-}$ was investigated on HCT-116 cells, grown in 96-well plates, 3000 cells in 90 μL culture medium per well. After 24h cell incubation, aliquots of $Ber^{+}Pal^{-}$ solutions, obtained by cascade dilution of a stock solution in ethanol, were added to the culture medium so that the final dye concentration ranged from 0.01 to 10 μM. Eight wells were considered for each concentration, and two controls were made (cells without dye and culture medium alone). After 4 day incubation, cell viability was evaluated by adding 10 μL of the cell proliferation reagent WST-1 (Roche) per well. After 2 to 3 hours, absorbance was measured at 450 nm using a Multiskan GO (Thermo Scientific) microplate reader spectrophotometer.

To study cellular uptake, cells were grown in Lab-Tek culture chambers, at least 36h before incubation with NPs. Then, they were incubated in the presence of NP suspensions: an aliquot (100 μL) of solutions of berberine salts at various concentrations was diluted in 900 μL of Opti-MEM and immediately spread on a monolayer of HCT-116 cells. Cells were then incubated for 1h at 37°C and the excess dye was washed away with Opti-MEM.

Dye localization was carried out on HCT-116 cells. Membrane labeling was performed by incubating cells in presence of 0.5 μg/mL CellMask® (1 μL solution at 5mg/mL in DMSO diluted 10000 folds with Opti-MEM) during 3 min at 37°C, then cells were washed twice with sterile PBS. MitoTracker® Red CMXRos solutions (Enzo Life Sciences) in specific buffer were applied on cells at the final concentration of 100 nM. Endoplasmic reticulum was stained using the ER-ID® Red (Enzo Life Sciences) dissolved in specific buffer (provided) at 1/3000 v/v before being applied on cells. After 15 min incubation at 37°C, cells were washed twice with sterile PBS.

Cells were systematically imaged in Opti-MEM (Life Technology). A Zeiss Axio Observer Z1 videomicroscope fitted with a CoolSnap HQ camera (Roper Scientific) was used (Imaging platform, ITAV), using suitable sets of filters (Red: λ_{ex} = 550 nm (±13 nm), λ_{em} = 605 nm (±35 nm); and GFP: λ_{ex} = 470 (±20 nm) or 438 nm (±12 nm), λ_{em} = 525 nm (±25 nm)) and a 40× objective. Image processing was performed using Metavue and Fiji softwares.

5. Conclusions

Delocalized lipophilic cations can appear as solid particles or dissolved compounds depending on the counter-ions they are associated to. The equilibrium between both forms is quite subtle and markedly influenced by the medium and the preparation procedures. This study underlined the importance of controlling the form under which the active compound appears and comes into contact with the cells. In the present case, it was not possible to say whether the intrinsic chemical properties of the TPB salt or the presence of submicrometric particles were responsible for the superior fluorescence intensity observed in the cells. But, in any case, using particles is at least as interesting as using dissolved compounds, with regard to cellular uptake. In view of the activity of berberine as both therapeutic and phototherapeutic agent, our results suggest that new investigations should be undertaken about the possibility to administer this compound as nano- and submicroscopic particles, in order to make the best of it. This type of study would deserve being extended to many other biologically-active DLCs and counter-ions.

The use of carrier-free nano- and submicrometric drug particles is a very promising approach for therapy and phototherapy.[3, 4] In parallel, pure organic dye particles open a new avenue for diagnosis.[30] In this context, the present study emphasized the interest of the

organic ion pair concept, which could allow DLCs to be used in a much more efficient and precise way for drug and dye delivery.

Acknowledgments

We are grateful to EuroNanoMed ERA-NET JTC2011 (FONDIAG project) for funding. We thank M. Laurent Weingarten (Service Commun de Microscopie Electronique de l'Institut de Chimie de Toulouse) for TEM images. The authors also acknowledge the support of the ITAV imaging facility and the TRI-Genotoul network.

Notes and references

[a] CNRS; ITAV-USR 3505; F31106 Toulouse, France.

[b] Université de Toulouse; ITAV-USR 3505; F31106 Toulouse, France.

[c] CNRS; IMRCP-UMR 5623; F31062 Toulouse, France.

[d] Université de Toulouse; IMRCP-UMR 5623; F31062 Toulouse, France.

* Corresponding author. Institut des Technologies Avancées en sciences du Vivant (ITAV), CNRS-USR 3505, Centre Pierre Potier, Oncopole, BP 50624, F31106 Toulouse, France. E-mail: suzanne.fery-forgues@itav.fr

†Electronic Supplementary Information (ESI) available: Volumes and concentrations of solutions used to prepare $Ber^{+}X^{-}$ salts using Protocol 1, solid-state spectroscopic characteristics of the berberine salts, UV-vis absorption spectra of berberine salts in acetonitrile, water and Opti-

MEM, transmission electron microscopy images, toxicity test for $Ber^{+}Pal^{-}$, microscopy images of cells incubated in the presence of $Ber^{+}TPB^{-}$. See DOI: 10.1039/b000000x/

1 J. S. Modica-Napolitano and J. R. Aprille, *Adv. Drug. Deliv. Rev.,* 2001, **49**, 63 and references therein.

2 K. Koya, Y. Li, H. Wang, T. Ukai, N. Tatsuta, M. Kawakami, T. Shishido and L. B. Chen, *Cancer Res.,* 1996, **56**, 538.

3 H. Kasai, T. Murakami, Y. Ikuta, Y. Koseki, K. Baba, H. Oikawa, H. Nakanishi, M. Okada, M. Shoji, M. Ueda, H. Imahori and M. Hashida, *Angew. Chem. Int. Ed.,* 2012, **51**, 10315; E. Merisko-Liversidge, P. Sarpotdar, J. Bruno, S. Hajj, L. Wei, N. Peltier, J. Rake, J. M. Shaw, S. Pugh, L. Polin, J. Jones, T. Corbett, E. Cooper and G. G. Liversidge, *Pharm. Res.,* 1996, **13**, 272; A. Jana, K. S. P. Devi, T. K. Maiti and N. D. P. Singh, *J. Am. Chem. Soc.,* 2012, **134**, 7656; R. Zhao, C. P. Hollis, H. Zhang, L. Sun, R. A. Gemeinhart and T. Li, *Mol. Pharmaceut.,* 2011, **8**, 1985.

4 K. Baba, H. E. Pudavar, I. Roy, T. Y. Ohulchanskyy, Y. H. Chen, R. K. Pandey and P. N. Prasad, *Mol. Pharmaceut.,* 2007, **4**, 289; E. Paszko, C. Ehrhardt, M. O. Senge, D. P. Kelleher and J. V. Reynolds, *Photodiagn. Photodyn. Ther.,* 2011, **8**, 14.

5 B. E. Rabinow, *Nat. Rev. Drug Discov.,* 2004, **3**, 785.

6 H. Yao, M. Yamashita and K. Kimura, *Langmuir,* 2009, **25**, 1131; Z. Ou, H. Yao and K. Kimura, *Bull. Chem. Soc. Jpn.,* 2007, **80**, 295; H. Yao and K. Ashiba, *RSC Advances,* 2011, **1**, 834.

7 J. Chahine, N. Saffon, M. Cantuel and S. Fery-Forgues. *Langmuir,* 2011, **27**, 2844.

8 S. Das, D. Bwambok, B. El-Zahab, J. Monk, S. L. de Rooy, S. Challa, M. Li, F. R. Hung, G. A. Baker and I. M. Warner, *Langmuir,* 2010, **26**, 12867.

9 S. Fery-Forgues, in *Aggregation-Induced Emission : Fundamentals,* (Eds: B. Z. Tang, A. Qin), John Wiley & Sons, Ltd., Singapore, ISBN 978-1-118-39430-4, 2014, pp. 104-124.

10 D. K. Bwambok, B. El-Zahab, S. K. Challa, M. Li, L. Chandler, G. A. Baker and I. M. Warner, *ACS Nano,* 2009, **3**, 3854.

11 P. K. S. Magut, S. Das, V. E. Fernand, J. Losso, K. McDonough, B. M. Naylor, S. Aggarwal and I. M. Warner, *J. Am. Chem. Soc.,* 2013, **135**, 15873.

12 D. S. Bhakuni and S. Jain, in: *The Alkaloids: Chemistry and Pharmacology*, Vol. 28, (Ed: A. Brossi), Academic Press, New York, 1986, pp. 95-174.

13 L. Grycová, J. Dostál and R. Marek, *Phytochemistry,* 2007, **68**, 150.

14 M. S. Arayne, N. Sultana and S. S. Bahadur, *Pak. J. Pharm. Sci.,* 2007, **20**, 83.

15 C. V. Diogo, N. G. Machado, I. A. Barbosa, T. L. Serafim, A. Burgeiro and P. J. Oliveira, *Curr. Drug Targets* 2011, **12**, 850; L. N. Xu, B. N. Lu, M. M. Hu, Y. W. Xu, X. Han, Y. Qi and J. Y. Peng, *Biocell,* 2012, **36**, 113.

16 S. M. Meeran, S. Katiyar and S. K. Katiyar, *Toxicol. Appl. Pharm.,* 2008, **229**, 33.

17 J. J. Inbaraj, B. M. Kukielczak, P. Bilski, S. L. Sandvik and C. F. Chignell, *Chem. Res. Toxicol.,* 2001, **14**, 1529.

18 K. Hirakawa and T. Hirano, *Photochem. Photobiol.,* 2008, **84**, 202.

19 S. Jantová, S. Letašiová, V. Brezová, L. Čipák and J. Lábaj, *J. Photochem. Photobiol. B,* 2006, **85**, 163.

20 M. S. Díaz, M. L. Freile and M. I. Gutiérrez, Solvent Effect on the UV/Vis *Photochem. Photobiol. Sci.,* 2009, **8**, 970.

21 A. Delgado-Camón, R. Garriga, E. Mateos, V. L. Cebolla, J. Galbàn, L. Membrado, S. de Marcos and E. M. Gálvez, *Chem. Phys. Lett.,* 2011, **501**, 547.

22 M. Megyesi and L. Biczók, *Chem. Phys. Lett.,* 2006, **424**, 71.

23 G. P. Schiemenz. *Org. Magn. Resonance,* 1973, **5**, 257.

24 T. Hinoue, Y. Shigenoi, M. Sugino, Y. Mizobe, I. Hisaki, M. Miyata and N. Tohnai, *Chem. Eur. J.,* 2012, **18**, 4634.

25 M. Breton, G. Prével, J. F. Audibert, R. Pansu, P. Tauc, B. Le Pioufle, O. Français, J. Fresnais, J. F. Berret and E. Ishow, *Phys. Chem. Chem. Phys.,* 2011, **13**, 13268.

26 S. E. A. Gratton, P. A. Ropp, P. D. Pohlhaus, J. C. Luft, V. J. Madden, M. E. Napier and J. M. DeSimone, *Proc. Nat. Acad. Sci. USA,* 2008, **105**, 11613.

27 C. V. Pereira, N. G. Machado and P. J. Oliveira, *Toxicol. Sci.* 2008, **105**, 408; G. C. Pereira, A. F. Branco, J. A. C. Matos, S. L. Pereira, D. Parke, E. L. Perkins, T. L. Serafim, V. A. Sardão, M. S. Santos, A. J. M. Moreno, J. Holy and P. J. Oliveira, *J. Pharmacol. Exp. Ther.,* 2007, **323**, 636; V. Mikeš and V. Dadák, *Biochim. Biophys. Acta,* 1983, **723**, 231.

28 L. Shen and H. F. Ji, *J. Photochem. Photobiol. B,* 2010, **99**, 154.

29 J. C. De Mello, F. H. Wittmann and R. H. Friend, *Adv. Mater.,* 1997, **9**, 230.

30 S. Fery-Forgues, *Nanoscale,* 2013**, 5**, 8428 and references therein.

Table of content entry

Fluorescent organic ion pairs based on berberine: Counter-ion effect on the formation of particles and on the uptake by colon cancer cells

Marine Soulié, Céline Frongia, Valérie Lobjois and Suzanne Fery-Forgues

Counter-ions modulate the fluorescence of beberine ion pairs in cells, this process being possibly linked to the formation of nanoparticles

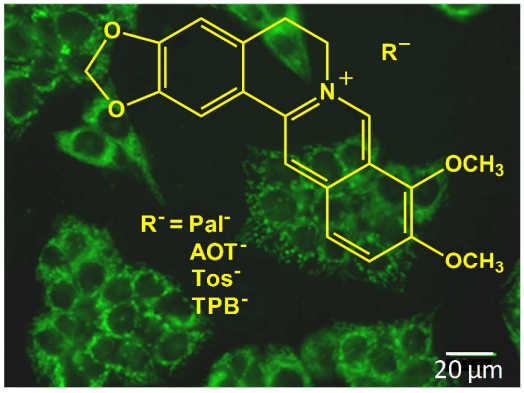

(The original figure in TIF is provided separately)

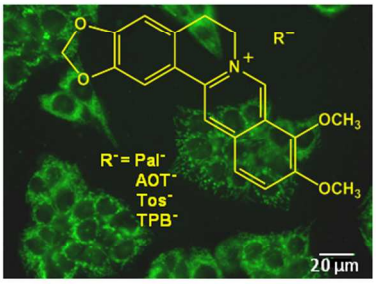

254x190mm (96 x 96 DPI)

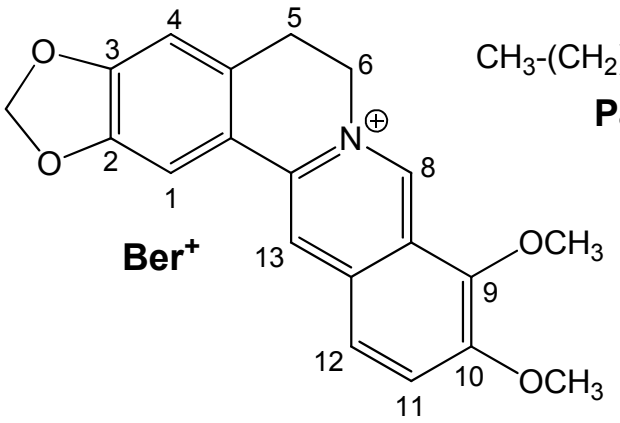

Ber^{+}

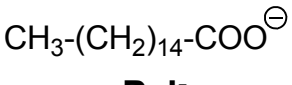

Pal^{-}

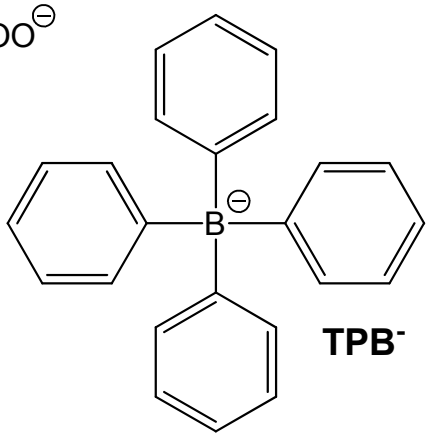

TPB^{-}

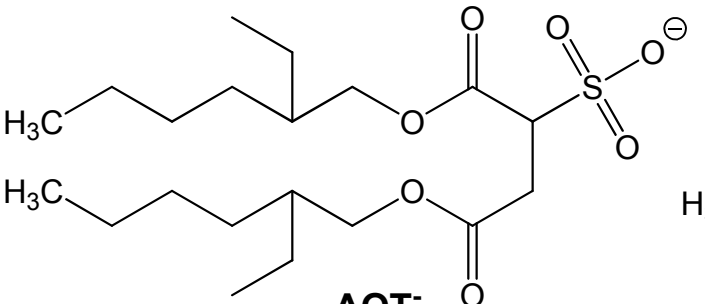

AOT^{-}

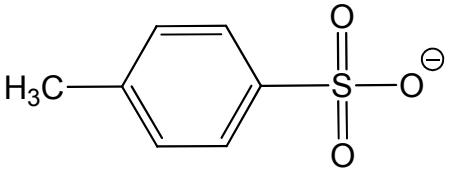

Tos^{-}

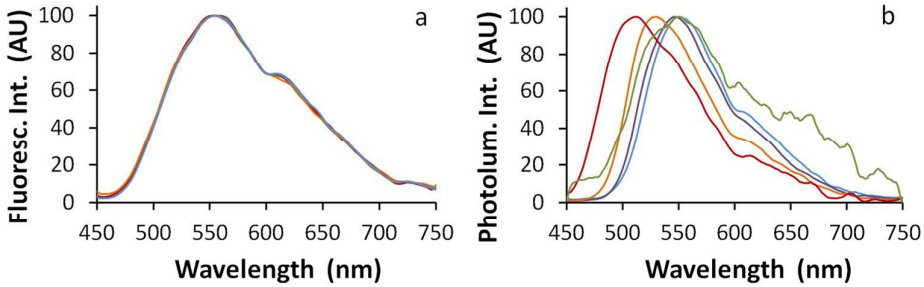
a
Fluoresc. Int. (AU)
100
80
60
40
20
0
450 500 550 600 650 700 750
Wavelength (nm)
b
Photolum. Int. (AU)
100
80
60
40
20
0
450 500 550 600 650 700 750
Wavelength (nm)

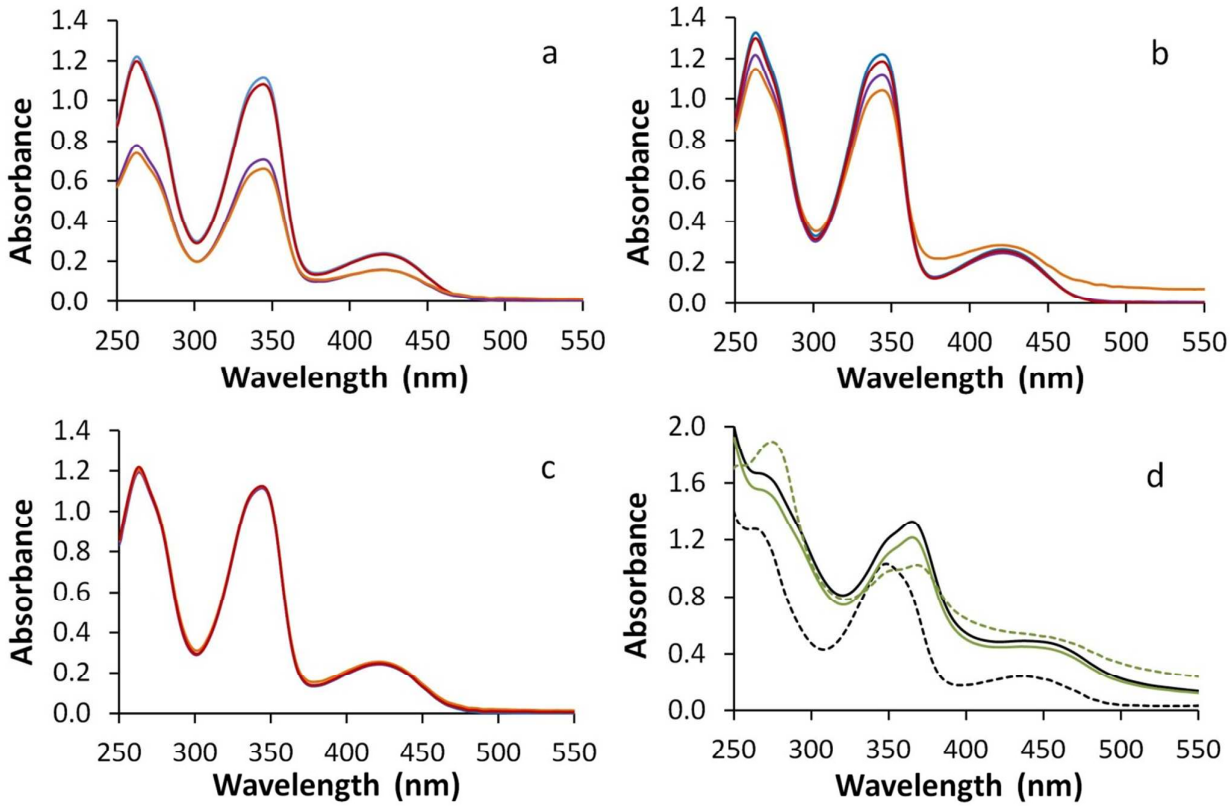
a
b
c
d
Absorbance
Wavelength (nm)
1.4
1.2
1.0
0.8
0.6
0.4
0.2
0.0
2.0
1.6
250
300
350
400
450
500
550

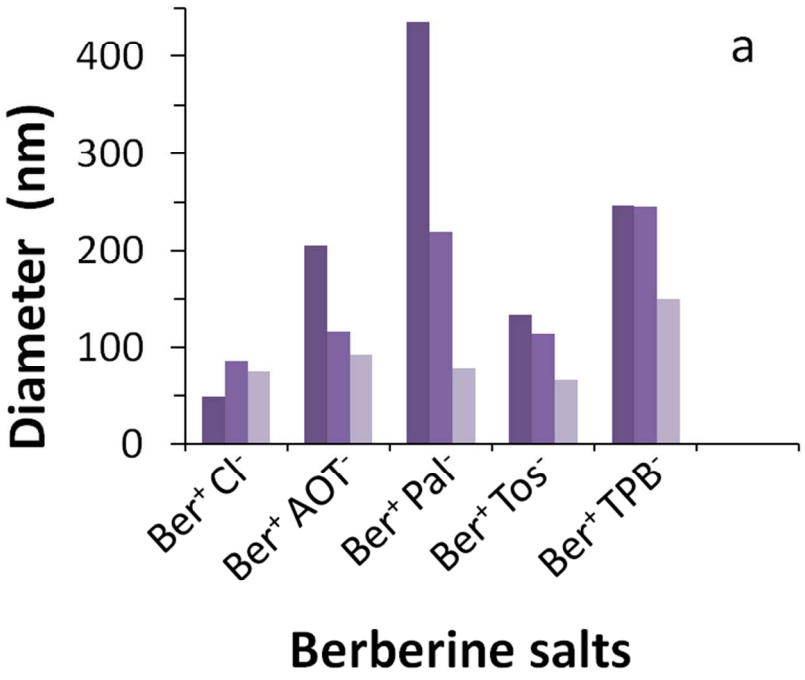

254x190mm (96 x 96 DPI)

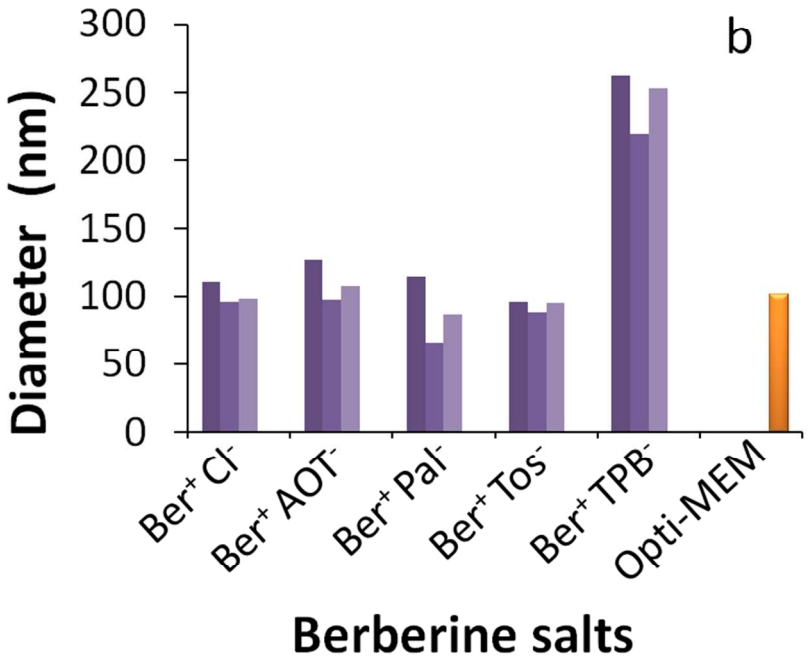

254x190mm (96 x 96 DPI)

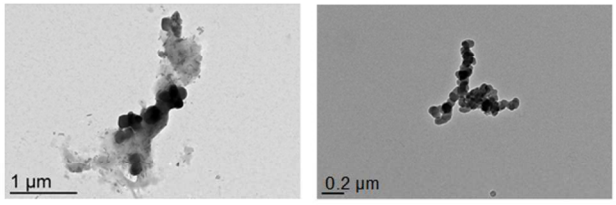

254x190mm (96 x 96 DPI)

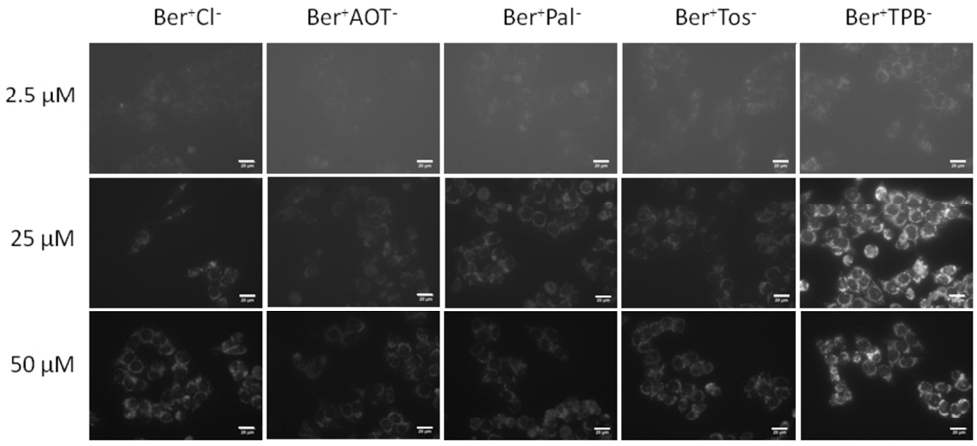

254x190mm (96 x 96 DPI)

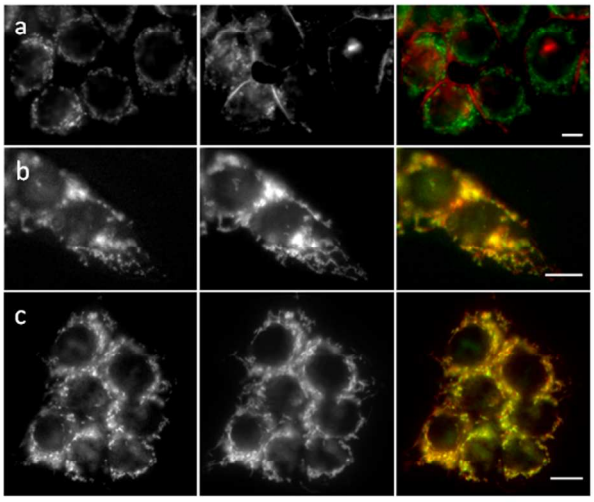

254x190mm (96 x 96 DPI)

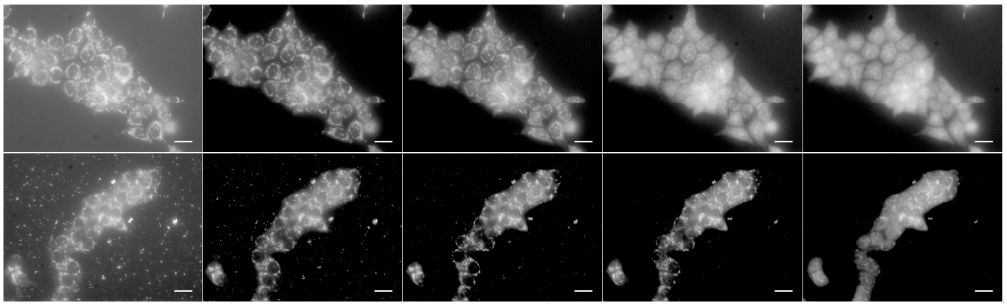

29493x8843mm (6 x 6 DPI)